Catheter-based ultrasound technology for image-guided thermal therapy: Current technology and applications

Vasant A. Salgaonkar and **Chris J. Diederich**

Dept. of Radiation Oncology, University of California San Francisco, 1600 Divisadero St. Suite H-1031, San Francisco, CA 94143, USA

Abstract

Catheter-based ultrasound (CBUS) is being applied to deliver minimally invasive thermal therapy to solid cancer tumors, benign tissue growth, vascular disease, and tissue remodeling. Compared to other energy modalities used in catheter-based surgical interventions, unique features of ultrasound result in conformable and precise energy delivery with high selectivity, fast treatment times, and larger treatment volumes. Here, a concise review of CBUS technology being currently utilized in animal and clinical studies or being developed for future applications is presented. CBUS devices have been categorized into interstitial, endoluminal and endovascular/cardiac applications. Basic applicator designs, site specific evaluations and possible treatment applications have been discussed in brief. Particular emphasis has been given on ablation studies that incorporate image-guidance for applicator placement, therapy monitoring, feedback control, and post-procedure assessment. Examples of devices included here span the entire spectrum of development cycle from preliminary simulation based design studies to implementation in clinical investigations. The use of CBUS under image guidance has the potential for significantly improving precision and applicability of thermal therapy delivery.

Keywords

catheter-based ultrasound; image guidance; thermal therapy; interstitial; endoluminal; endovascular

1. Introduction

Energy-based thermal therapies are used in minimally-invasive treatments for a wide range of medical interventions. Some exciting treatment areas include solid cancer tumors, benign tissue abnormalities, tissue remodeling and repair, vascular stasis, cosmesis, cardiovascular applications, and brain surgery. This review reports recent developments in catheter-based ultrasound (CBUS) technology for hyperthermia and thermal ablation. Thermal ablation procedures involve localized heat deposition to achieve target temperatures of 52 - 100 °C for short durations which result in irreversible coagulation, protein denaturation, necrosis and in some cases eventual reabsorption and remodeling of the treated tissue [1]. Hyperthermia treatments employ temperature elevations between 39 – 45 °C for typical

durations of 30-60 min. Hyperthermia is utilized as an adjunct to radiation and chemotherapy for cancer. It provides treatment enhancement through mechanisms such as improvement in tumor oxygenation, decrease in radiation resistance of the tumor cells, better chemotherapy delivery and increased cellular cytotoxicity [2].

Medical devices clinically used for administering thermal therapy can utilize several different energy sources such as radiofrequency (RF) currents, microwaves (MW), laser, ultrasound, and thermal conduction sources. They consist of configurations built for external or extracorporeal, interstitial or percutaneous, and endoluminal or endocavity placement [1]. Ultrasound (US) as an energy modality offers several advantages over other competing technologies. This includes improved energy penetration for treating deep targets, small wavelengths that enable better focusing, and precise control of energy deposition shape and location [1, 3]. Extracorporeal and intracavitary high-intensity focused ultrasound (HIFU) devices under image guidance are increasingly being used in ablation treatments [4], and demonstrate advantages of ultrasound energy. Although precise, HIFU ablation requires sequential coagulation of small overlapping volumes to cumulatively treat a larger target. This involves multiple individual short-time, high-power sonications. Target coverage is achieved through mechanical or electrical translation of the HIFU beam through complicated device designs. Treatment times are long and can even extend to several hours. Plus, the treatments are susceptible to complication from *in vivo* motion and near-field heating. As an alternative to HIFU, CBUS devices are positioned directly within or adjacent to the target, and can coagulate large continuous volumes. The applicators require less manipulation after deployment. Typical treatments may require 10 – 30 min of heating time. CBUS procedures are more invasive than external HIFU but also lead to better energy localization.

For this review, the CBUS device classification includes [1] interstitial applicators directly placed within the target volume, [2] endoluminal devices placed within lumen or body cavities and [3] endovascular or cardiac applicators placed through or within major blood vessels. These are included in sections 2 – 4 respectively. These sections contain examples of device designs and treatment applications. A summary of selected CBUS applicators, their design features, performance and clinical utilization can be found in Tables 1 – 3. The devices reviewed here have designs with transducer assemblies mounted on small catheters and hence large endorectal ultrasound applicators are excluded. For brevity, CBUS applicators already integrated with or amenable for use with image guidance methods are considered. The review uses examples from ongoing or recent investigations. Interventional image guidance methods such as magnetic resonance imaging (MRI) [1, 5, 6], US [1, 7], computed tomography (CT) [1, 7] and electromagnetic (EM) [1] tracking have been included in section 5. It should be noted that many of these techniques are successfully employed to monitor thermal therapy with energy modalities other than CBUS. Section 6 summarizes future prospects of CBUS technology in academia and industry.

2. Interstitial CBUS

2.1. Overview of interstitial applicator designs

Typical design of interstitial ultrasound applicators consists of one or more transducers lined in form of a linear array at the tip of a thin supporting shaft. One applicator configuration which has been utilized in several investigations consists of tubular transducers [1, 8-10]. The transducer tubes can be longitudinally scored to create independent angular sectors, which are powered independently. This configuration allows for controlled power deposition in angle and length. The sector angles can vary between 90°- 360°. A bidirectional applicator can be created by wiring both opposing 180° sectors. Transducer frequencies can range from 3 – 10 MHz (majority of devices utilize 6 – 8 MHz), outer diameters between 1.5 – 2.4 mm, transducer lengths between 5 – 15 mm, with 3-4 transducer segments total. They can either be coupled to the tissue directly with internal cooling or be placed inside a cooling catheter (Figure 1a).

In a more complex configuration, electronic rotational control of acoustic energy deposition was achieved with a multi-faced device (distal tip shaped like a block with 7 sides) consisting of multiple arrays of planar transducers (56 elements, 6 MHz), with independent control of power output from each face. This multi-faced device has an outer diameter of 3.2 mm, an integrated cooling channel, and is deployed within a 4.8 mm diameter sheath for coupling and water flow return [11]. This design, as well as the tubular-element CBUS applicators discussed earlier, can obtain angular and axial control of ablation without mechanical manipulation of the device, which can facilitate MR guidance and simplify treatment delivery.

Dual mode interstitial ultrasound applicators have also been reported in the literature. They may be more complicated in design, construction and hardware requirements but offer potential for real-time image-guided treatment with the same device utilized for both tasks, enabling near perfect co-registration between the treated and monitored volume. One design consists of a linear array of 32 flat rectangular transducers (3.1 or 4.8 MHz, array dimensions: 2.3×49 mm^2). Therapy is delivered by the central 16 elements and B-mode images are captured by the complete 32-element aperture. Short imaging cycles are periodically interleaved with therapy sonications [12-15]. This image-ablate array was designed for percutaneous and laparoscopic placement, and was cooled/coupled by an outer cooling balloon. Another design for a dual-mode applicator (Figure 1b) consisted of a 5-element linear array (5 – 6 MHz). Therapy was delivered using all 5 elements. Therapy sonications were paused for imaging with the central element. The central element was operated in pulse-echo mode to acquire A-line data. Therapy and imaging cycles were interleaved. While imaging, the applicator was oscillated with a servo-motor to span a 140° imaging plane orthogonal to the applicator axis [16-18]. This design was adapted from a simpler single-element dual-mode configuration [19].

2.2. Treatment sites: Interstitial applicators

Spine—Minimally invasive ablation treatment for chronic back pain may involve necrosis of nerve fibers and collagen shrinkage near the vertebral annular wall. Commonly performed

by RF or conductive heating, studies have shown the feasibility of applying interstitial ultrasound with directional tubular applicators. Experiments in cadaveric spine segments [20] and *in vivo* ovine [21] have shown the ability to selectively target the annular wall nucleus, shrink collagen (high-temperature exposures > 70 °C) and ablate nociceptor fibers (low-temperature exposures ∼52 °C) with minimal degradation of mechanical and cellular parameters of the intravertebral disc. *In vivo* ablation of spinal or paraspinal VX2 tumors in rabbits was also demonstrated using similar transducers where a bone biopsy needle was placed into the center of the tumor and an interstitial ultrasound applicator was inserted through the central channel [22]. Tumor destruction was identified through histological staining. Simulation and *ex vivo* tissue studies were reported recently where performance of such interstitial ultrasound devices was characterized across a range of design parameters to explore treatments options for tumors in different locations and sizes [23]. Patient specific modeling studies were also conducted to investigate treatment delivery strategies [24], demonstrating that the interaction of ultrasound energy with surrounding bone can be used to enhance localization of therapy.

Liver—nterstitial ultrasound with its inherent advantages in terms of conformable energy delivery and potential for larger treatment volumes has been the focus of several studies to develop methods for percutaneous ablation of large non-resectable liver tumors. This includes *ex vivo* ablation studies [12, 16, 25-29], *in vivo* animal [18, 30, 31], and implanted tumor models [14, 15]. Dual-mode applicators have been applied for US-guided ablations [12, 14-19, 25]. Studies have also included the use of multi-applicator implants with tubular transducer devices for conformal therapy even under oblique insertion [26], demonstrating advantages over similar interstitial RF and microwave applicators.

Pelvic diseases—Interstitial ultrasound applicators can be used to deliver localized or focal therapy for treating prostate cancer. The feasibility of focal ablation with tubular transducer CBUS applicators has been demonstrated through numerical simulations [32, 33] and animal studies [34-37]. An example of prostate ablation with percutaneously placed CBUS applicators is shown in Figure 1c for an *in vivo* canine model. Similar CBUS tubular applicators were used in a clinical pilot study to deliver hyperthermia in conjunction with HDR brachytherapy for advanced prostate and cervical cancer [38]. Also, studies related to hyperthermia treatment schema [38, 39] and optimization with CBUS tubular applicators have been reported [40, 41]. Another potential application is the treatment of large uterine fibroids. Initial studies performed on surgically excised human fibroid showed an ability to ablate diameters approaching 4 cm and volumes greater than 45 cm^3 in less than 15 min with a single needle insertion [42].

Brain—The feasibility of interstitial ultrasound ablation of brain tumors under MR guidance was demonstrated through *in vivo* canine models with implanted transmissible venereal tumors in the brain (Figure 1d). Directional tubular interstitial applicators (7.1 – 8.15 MHz, 1.8-2.4 mm OD) with internal cooling and integrated catheter cooling were utilized to demonstrate shaped directional thermal coagulation of tumors and establish lethal thermal dose of 50 equivalent minutes at 43 °C within brain tissue. Ablative necrosis was observed in 1.5 – 4.0 cm^3 volumes [10, 37], with good agreement between histological

findings and lethal thermal dose. Controlled ablation of brain tissue was also demonstrated using multi-faced interstitial applicators in *ex vivo* experiments [11]. In a recent study aimed at showing initial feasibility, a 6-mm OD rotating endoluminal applicator was interstitially placed within an *in vivo* porcine brain to perform ablations [43] and evaluate general performance under MR thermometry feedback control, demonstrating a high degree of conformal delivery.

3. Endoluminal CBUS

3.1. Overview of endoluminal applicator designs

Endoluminal devices are designed for placement within body cavities and lumens such as the gastro-intestinal (GI) tract, esophagus, or genito-urinary (GU) tract. Typically they can be larger in size than interstitial applicators and can either be housed on flexible or steerable catheters, or on rigid shafts depending upon the application. A larger footprint allows the use of multiple transducer elements, sometimes also in form of phased arrays. Unlike interstitial devices, they are not placed directly within the tumor, but adjacent to or in close proximity of the target. This delivery strategy also necessitates effective coupling and a cooling to ensure sufficient acoustic energy delivery to the target with minimal thermal deposition in the intervening tissue.

Transurethral catheter-based ultrasound applicators have been devised for treating prostate diseases. One CBUS design consists of large tubular transducers (PZT4-8, 6-8 MHz, 2.5-3.5 mm outer diameter, 6-10 mm length segments) housed within a cooling balloon and connected to custom-designed multi-lumen Pebax (a flexible medical grade polymer) catheters (4-6 mm OD). The catheter body contains channels for water flow, RF power feed lines and wiring for any MRI active tracking coils (used in device localization). Depending on the application, applicator designs included a single active sector of 90°[44, 45] or 180°[35, 45-47], or two active sectors of 120°[45, 48-50] each. The typical design consisted of two or three transducer tubes of 6 - 10 mm. The distal end of the applicator had a distensible C-flex balloon for locking the device at the bladder neck. The devices were designed to be compatible with the MRI environment [35]. This general transducer assembly configuration was also adapted to develop an endocervical applicator with 360°, 2×180° and 3×120° sectors coupled to the tissue from within a rigid PET catheter [38-40, 51]. A similar catheter assembly was also used for applicators with flat rectangular or curvilinear (lightly focused) transducers, which could be sequentially rotated with an MR compatible stepper motor to sweep and generate larger conformal ablation volumes [44, 52].

Another design, also for transurethral therapy, consists of one or more rectangular planar transducers (8 – 9 MHz] mounted on a rigid brass shaft and connected to a rotational motor and positioning system [53-55]. Cooling water is circulated through the applicator and over the transducers which are covered with a plastic housing and polyester membrane that serves as an acoustic window. A similar configuration also employs multi-frequency transducers which are created by adding high-impedance matching layers to a single PZT transducer crystal which enables it to resonate efficiently at two distinct frequencies [56]. Treatment depth can be varied by changing the operating frequency which in turn controls ultrasound penetration. Such applicators can also have multiple planar transducers arranged on a rigid

shaft in form for a linear array. The typical transducer width is 4 – 5 mm and the overall applicator diameter is ∼6.4 mm. A similar design with a single transducer element (10.6 MHz, 6×10 mm^2) was also reported by Lafon *et al*. [57].

Several devices have been reported in the literature for transesophageal access [58-66]. Some have a flat or curved single transducer element (∼ 2 - 10 MHz), water-tight coupling balloons and flexible shafts for rotation control. Simulation and preliminary studies have been reported for phased array devices for such applicators [67-72]. Some of these designs also have integrated MR imaging coils [60, 61] or ultrasound imaging probes [62, 63].

3.2. Treatment sites: Endoluminal applicators

Pelvic disease—Endoluminal ultrasound has been used for transurethral prostate ablation (Figure 2a, b). Such transurethral applicators have been developed for focal prostate cancer therapy or for treating benign prostatic hyperplasia (BPH). This may be achieved through rotational sweeping of devices with planar or curvilinear transducers, or stationary devices with sectored tubular transducers. Simulation and preliminary *ex vivo* experiments [57, 73-79], *in vivo* animal models [44, 46, 47, 52, 80-82], and clinical cases [55] have been described in the literature and show successful implementation of this ablation technique. Ablation localized to the transition zone has also been demonstrated in a canine model *in vivo* with sectored tubular applicators as a potential treatment option for BPH [48, 49]. Endocervical tubular applicators [39, 51] have been successfully utilized to deliver hyperthermia to tumors in the cervix as an adjuvant treatment to radiotherapy (Figure 2c). During a pilot clinical hyperthermia study, multi-sectored ultrasound applicators were deployed through a tandem catheter placed within the uterine cervix for brachytherapy procedures [38].

Ablation through GI tract—Ablation of targets through the esophagus for treating esophageal tumors was demonstrated through *in vivo* porcine [83] and pilot clinical studies [59]. A 4-patient pilot study is reported for the ablation of tumors in the esophagus with a transesophageal applicator and feasibility of creating highly-demarcated ablative lesions in the esophagus was indicated [59]. Liver ablation using transgastric ultrasound was also demonstrated *in vivo* in swine models using an endoscopic device, and it was possible to create small lesions in the liver [58, 62]. Intraductal ablation of tumors in the digestive tract and billiary duct has been studied in swine models where small diameter devices (3.8 – 4 mm) have been deployed within working channels of endoscopes [84, 85]. Further, transesophageal devices have been designed for targeted ablation of the left atrium for treatment of atrial fibrillation (Figure 2d). Some recent studies include *in vivo* swine models with atrial and ventricular myocardial ablations [72], *ex vivo* pig hearts [63, 64, 86], and simulation and device design [68-70].

4. Endovascular And Cardiac CBUS

4.1. Overview of endovascular applicator designs

Many general device configurations discussed in the previous sections have been adopted for endovascular and cardiac applications. Here, endovascular CBUS implies devices which

are placed directly within blood vessels to target nearby or surrounding structures. In typical interventions such devices are deployed through steerable catheter sheaths and introducers that are themselves positioned percutaneously for accessing the vascular system. These applicators tend to have lumens to accommodate guide-wires, allowing for over-wire advancement and positioning. Similar to some of the designs discussed earlier, these applicators also tend to have coupling/cooling balloons or sheaths and, as necessitated for this application, flexible and steerable device bodies.

Earlier CBUS applicators for endocardial ablation consisted of single tubular or planar radiators [87, 88] mounted on the distal catheter, with later versions including an expandable silicone cooling balloon and catheter design for over the wire placement in the pulmonary veins (PV) for circumferential ablation [89]. Advancing this design, a parabolic reflector balloon with a partial gas filled layer was incorporated to produce a tip firing annular ablation pattern from the tubular PZT to better target the PV. The device has a deflectable tip for improved maneuverability and can be positioned from within an 8-French catheter [90-93]. These devices are also called HIFU-BC (for HIFU balloon catheter) in the literature [94-96]. A catheter with a front facing planar phased array at the tip, 112-element 2-D phased array (5 MHz), deployed from within a 12-French catheter has been reported for myocardial ablation [97].

Endovascular devices with single tubular transducers at the tip have also found applications in renal denervation. The device design consists of a single tubular transducer (~9 MHz, 6 mm length) centered within an acoustically transparent balloon for cooling and coupling of the acoustic energy. It is designed for insertion over a guide-wire through a 6-French catheter, and can be steered to the renal artery via a femoral access [98, 99].

4.2. Treatment Sites: Endovascular applicators

Cardiac—Some endovascular devices have also been used for treating atrial fibrillation (AF). One possible treatment involves ablating the thin muscles and nerve pathways around the pulmonary vein ostium in a circumferential manner (Figure 3). Studies have reported this procedure in canine models and in patients. The applicators are inserted through the septum and seated near the pulmonary vein ostium to perform these ablations. A canine model study reports that ablations were successfully delivered with the parabolic reflective applicator discussed earlier (section 4.1). The treatment time was 60 – 90 s at 40 W of applied power [90]. Clinical studies have been performed with such CBUS devices. Treatment of AF was indicated in some patients. No evidence of PV stenosis was detected however significant adverse events were reported including damage to the esophagus and phrenic nerve [91, 95, 96]. In consideration of pulmonary vein ablation, the enhanced penetration of ultrasound energy through the thin target region of the PV and the proximity of critical sensitive tissue structures, combined with the lack of image-guidance or real-time monitoring of treatment, leads to serious safety issues, and contraindicates clinical use of this approach [100].

There have been several studies which employ the Cox-Maze procedure for treating atrial fibrillation using commercial devices. In some of these studies, a flexible acoustically transparent catheter is inserted in the pericardial space following a sternotomy and then this

catheter is wrapped around the atrium by displacing the pulmonary veins. The catheter is then cinched around the heart and a HIFU transducer is advanced through the hollow catheter tube to create lesions in the heart muscle. This is an open epicardial procedure and does not technically use an endovascular CBUS catheter, but some studies are included here for completeness [101-103].

Renal Vasculature—Hyperactivity of the sympathetic nervous system can be a factor contributing to drug-resistant hypertension. Thermal ablation of nerves circumferentially surrounding the renal artery is a potential treatment that has gained traction recently using RF ablation catheters and external HIFU approaches. Enthusiasm for this procedure has diminished recently due to a recent randomized trial that showed no significant reduction in blood pressure using the Symplicity RF ablation device [104]. It should be noted that the RF catheter procedure as applied does not penetrate significantly and produces only 4-6 non-contiguous thermal lesions around the renal artery. This most likely, prevents thorough destruction of the sympathetic nerves. Recent studies have reported this procedure using small endovascular CBUS applicators, designed to be seated within the distal renal artery with inflation of an expandable water-cooled balloon. Figure 4 depicts a renal denervation applicator and example circumferential coagulation pattern in tissue phantom. A detailed *in vivo* swine study was reported to characterize the performance of CBUS applicators at different power-time exposure combinations. Circumferential ablation of nerves and tissue surrounding the renal artery was successfully demonstrated while sparing the renal artery itself [99]. In a pilot clinical study, the applicator was placed within the renal artery through a standard femoral access. Fifty second long ablations were performed at 25 – 30 W in three locations of the distal renal artery in 11 patients. The patients exhibited a statistically significant drop in blood pressure which was sustained at three months follow-up [98]. The circumferential and penetrating heating patterns of CBUS in this application present significant advantages over the RF devices currently being applied.

5. Image Guidance

CBUS devices reported here have been successfully integrated with radiological imaging modalities such as MRI, US and CT/Fluoroscopy to demonstrate image-guided thermal therapy. Each of these modalities can be used for target localization and device placement. US and MRI have also been used for tracking ablation progress in real-time and for damage assessment post treatment. Further details of representative studies are given next.

CT or fluoroscopy is an effective imaging modality for placement of interstitial ultrasound catheters and it has been employed in studies that focus on treatments near the spine [20, 21]. CT images of brachytherapy implants are also used to plan interstitial CBUS hyperthermia applied through the implanted catheters [38, 40, 41]. Electromagnetic tracking methods have been integrated with cone-beam CT for guiding needle placement for interstitial ultrasound ablation [105]. For endovascular applications, fluoroscopy and CT are often used to place the ablation applicators using standard angiographic techniques in the heart [90, 91] and kidneys [98, 99].

Ultrasound image-guidance has been applied to monitor tissue coagulation and placement of CBUS probes. Tissue coagulation can be monitored by identifying changes in echogenicity [57, 59], Doppler signals [57], backscatter [18], stiffness [16, 19, 106, 107] and echo-decorrelation[14, 15]. US imaging has also been successfully implemented to guide and position interstitial CBUS devices. For example, endorectal US can be used to implant catheters for US hyperthermia to the prostate [38], and 3D US probes have been utilized in the placement of mechanically steerable CBUS applicators [108]. Some recent efforts have combined electromagnetic tracking with US imaging to co-register applicator position with anatomy for potential robotic placement [106, 109]. Ultrasound guided endoscopic ultrasound ablation procedures have been reported for clinical esophageal tumor ablation [59] and in liver ablation studies [62]. Similar technology development was conducted for transesophageal cardiac ablation with an imaging transducer centered and integrated within the therapy array for US-guided target localization [63, 86]. There have been attempts to use intra-cardiac ultrasound imaging to guide RF-based thermal ablation procedures for treating atrial fibrillation [110], which may have potential for guiding CBUS too.

MR-guided CBUS consists of MR thermometry with proton resonance shift imaging [36, 111], real-time temperature-based feedback control [43], and post ablation damage assessment through contrast enhanced imaging [10, 37, 43, 111]. In particular, MR temperature imaging (MRTI] which has been a valuable tool in clinical translation of HIFU ablation technology [5, 112] has also found applications in CBUS therapy monitoring. MR-guided interstitial CBUS has been demonstrated in brain ablation in canine [10, 37] and porcine models [43] *in vivo*. It was also reported for monitoring of *in vivo* ablations in porcine liver [111] and canine prostate [36]. Several examples of successful implementation of transurethral CBUS ablation of prostate with multi-planar PRFS-based MRTI are reported in the literature [36, 46-48, 50, 52-55, 81, 82]. Ancillary studies related to diffusion-weighted imaging [80] and refinement of MR techniques for motion compensation have also resulted from similar work [76, 113, 114]. MR thermometry techniques have also been explored for monitoring endoscopic ablation of liver and pancreatic tumors [58, 65, 66]. MRTI-based feedback control has been demonstrated using schemes such as proportional integral [43, 74, 75, 77, 78] and self-tuning [78] and robust predictive [77] controllers. The integration of MRTI with the spatial control and conformal heating capabilities of CBUS holds promise for delivery of accurate and precise thermal therapies under real-time treatment control. However, MRTI for CBUS procedures can be more challenging when compared to MR-guided HIFU. MR temperature imaging can be sensitive to susceptibility artifacts from the inserted devices themselves, movement of organs or target regions during respiration or cardiac cycle, adjacent organs or gas (lung, bowel) generating susceptibility artifacts, or phase drift over the longer duration procedure times. Recent investigations described above have demonstrated that the artifacts generated from the devices themselves can be minimized with proper selection of MR compatible materials and fabrication techniques, so that regions as close as 1-3 mm from the applicator extending to the outer treatment boundary can be effectively monitored [49, 55, 82]. Tissue motion related errors can be compensated through multi-baseline or multi-reference imaging [76, 115-117]. Background or baseline phase drift errors can be compensated by tracking phase changes outside the heated region [115]. As an example, these approaches have been shown to be

accurate for 10-30 min CBUS procedures *in vivo* [37, 45, 54] and in clinical prostate ablation [55]. Similar long term MRTI strategies have been investigated for long duration pelvic hyperthermia with electromagnetic heating sources [118-122] and clinical RF ablation of liver [123], and could readily be adapted for CBUS hyperthermia and longer duration ablations. In some target regions organ movement during the respiratory cycle could be restrained by the physical placement and constraint of the CBUS applicator(s), which can maintain targeting from within or adjacent to the target and avoid MRTI errors. However, in situations where movement remains significant then respiratory gating of the MRTI acquisition and possibly breath holds would need to be considered, such as currently performed for HIFU of targets within liver or pancreas that undergo substantial displacement [112, 115]. The presence of gas in organs such as bowel, rectum or lungs can also lead to changes in local magnetic susceptibility and hamper the quality of MRTI during CBUS procedures. New spatiotemporal filtering techniques are being developed to account for susceptibility changes induced by the movement of air bubbles in the rectum [76].

6. Looking Ahead

In general CBUS technology has many advantages over alternative energy modalities, most significant being the ability of ultrasound to afford customized and spatially controlled energy placement. Additionally, CBUS is compatible with many existing image guidance and monitoring techniques. The development, clinical implementation, and commercialization of site and disease specific CBUS devices remain challenging. However CBUS technology has been or is currently under development at academic research institutions and commercial entities. Some examples of commercialized devices or those of significant commercial interest include: transurethral devices that originated in the academic domain are being further developed by companies such as Profound Medical [55] and Phillips [82]; dual-mode US arrays for percutaneous and laparoscopic applications as developed by Guided Therapy Systems [12, 25]; large split-beam HIFU devices developed by Sonacare Medical for laparoscopic ablations [124]; a 7-sided interstitial device reported by Canney et al. [11] for brain ablation is of commercial interest to Carthera; HIFU-BC catheters developed by Atrionix/Johnson & Johnson [91] and ProRhythm[95, 96] to treat atrial fibrillation by ablating tissue surrounding the pulmonary vein; and Recor Medical has developed and clinically evaluated CBUS for renal denervation in the treatment of hypertension [98, 99]. Motivating factors in support of development of CBUS technology may include: has the potential to deliver fast and highly conformable volumetric ablation with short procedure times and less resource intensive than many currently used devices; devices of the type which will be in direct contact with the target tissue may be able to follow the 510k route for FDA approval for use and marketing, which requires significantly less time and expense than the alternative Pre-Market Approval (PMA); similar to HIFU, CBUS is amenable to image guidance and monitoring platforms; deployment of CBUS procedures fit closely within existing standards of practice for interventional radiologists and surgeons implementing thermal therapy. In looking ahead, CBUS technology has many possible advantages over existing technology that will foster additional academic and commercial development of these devices as the field of image-guided ultrasound thermal therapy continues to move forward.

Acknowledgments

References

1. Diederich CJ. Thermal ablation and high-temperature thermal therapy: overview of technology and clinical implementation. International journal of hyperthermia. 2005; 21(8):745–753. [PubMed: 16338857]

2. Hildebrandt B, Wust P, Ahlers O, Dieing A, Sreenivasa G, Kerner T, et al. The cellular and molecular basis of hyperthermia. Critical reviews in oncology/hematology. 2002; 43(1):33–56. [PubMed: 12098606]

3. Lafon C, Melodelima D, Salomir R, Chapelon JY. Interstitial devices for minimally invasive thermal ablation by high-intensity ultrasound. International Journal of Hyperthermia. 2007; 23(2): 153–163. [PubMed: 17578339]

4. Schlesinger D, Benedict S, Diederich C, Gedroyc W, Klibanov A, Larner J. MR-guided focused ultrasound surgery, present and future. Medical physics. 2013; 40(8):080901. [PubMed: 23927296]

5. Hynynen K. MRI-guided focused ultrasound treatments. Ultrasonics. 2010; 50(2):221–229. [PubMed: 19818981]

6. Kennedy JE. High-intensity focused ultrasound in the treatment of solid tumours. Nature reviews cancer. 2005; 5(4):321–327. [PubMed: 15776004]

7. Goldberg SN, Grassi CJ, Cardella JF, Charboneau JW, Dodd IIIGD, Dupuy DE, et al. Image-guided tumor ablation: standardization of terminology and reporting criteria. Journal of Vascular and Interventional Radiology. 2009; 20(7):S377–S390. [PubMed: 19560026]

8. Diederich C. Ultrasound applicators with integrated catheter-cooling for interstitial hyperthermia: theory and preliminary experiments. International journal of hyperthermia. 1996; 12(2):279–297. [PubMed: 8926395]

9. Lee RJ, Buchanan M, Kleine LJ, Hynynen K. Arrays of multielement ultrasound applicators for interstitial hyperthermia. Biomedical Engineering, IEEE Transactions on. 1999; 46(7):880–890.

10. Kangasniemi M, Diederich CJ, Price D, Roger E, Stafford RJ, Schomer DF, et al. Multiplanar MR temperature-sensitive imaging of cerebral thermal treatment using interstitial ultrasound applicators in a canine model. Journal of Magnetic Resonance Imaging. 2002; 16(5):522–531. [PubMed: 12412028]

11. Canney MS, Chavrier F, Tsysar S, Chapelon JY, Lafon C, Carpentier A. A multi-element interstitial ultrasound applicator for the thermal therapy of brain tumors. The Journal of the Acoustical Society of America. 2013; 134(2):1647–1655. [PubMed: 23927205]

12. Makin IRS, Mast TD, Faidi W, Runk MM, Barthe PG, Slayton MH. Miniaturized ultrasound arrays for interstitial ablation and imaging. Ultrasound in medicine & biology. 2005; 31(11):1539–1550. [PubMed: 16286031]

13. Mast TD, Pucke DP, Subramanian SE, Bowlus WJ, Rudich SM, Buell JF. Ultrasound monitoring of in vitro radio frequency ablation by echo decorrelation imaging. Journal of Ultrasound in Medicine. 2008; 27(12):1685–1697. [PubMed: 19022994]

14. Mast TD, Barthe PG, Makin IRS, Slayton MH, Karunakaran CP, Burgess MT, et al. Treatment of Rabbit Liver Cancer *In Vivo* Using Miniaturized Image-Ablate Ultrasound Arrays. Ultrasound in medicine & biology. 2011; 37(10):1609–1621. [PubMed: 21821349]

15. Subramanian S, Rudich SM, Alqadah A, Karunakaran CP, Rao MB, Mast TD. *In Vivo* Thermal Ablation Monitoring Using Ultrasound Echo Decorrelation Imaging. Ultrasound in medicine & biology. 2014; 40(1):102–114. [PubMed: 24239361]

16. Bouchoux G, Owen N, Chavrier F, Berriet R, Fleury G, Chapelon JY, et al. Interstitial thermal ablation with a fast rotating dual-mode transducer. Ultrasonics, Ferroelectrics and Frequency Control, IEEE Transactions on. 2010; 57(5):1066–1095.

17. Owen N, Chapelon J, Bouchoux G, Berriet R, Fleury G, Lafon C. Dual-mode transducers for ultrasound imaging and thermal therapy. Ultrasonics. 2010; 50(2):216–220. [PubMed: 19758673]

18. Owen NR, Bouchoux G, Seket B, Murillo-Rincon A, Merouche S, Birer A, et al. In vivo evaluation of a mechanically oscillating dual-mode applicator for ultrasound imaging and thermal ablation. Biomedical Engineering, IEEE Transactions on. 2010; 57(1):80–92.

19. Bouchoux G, Lafon C, Berriet R, Chapelon JY, Fleury G, Cathignol D. Dual-mode ultrasound transducer for image-guided interstitial thermal therapy. Ultrasound in medicine & biology. 2008; 34(4):607–616. [PubMed: 18055099]

20. Nau WH, Diederich CJ, Shu R. Feasibility of using interstitial ultrasound for intradiscal thermal therapy: a study in human cadaver lumbar discs. Physics in medicine and biology. 2005; 50(12): 2807. [PubMed: 15930604]

21. Bass EC, Nau WH, Diederich CJ, Liebenberg E, Shu R, Pellegrino R, et al. Intradiscal thermal therapy does not stimulate biologic remodeling in an in vivo sheep model. Spine. 2006; 31(2):139–145. [PubMed: 16418631]

22. Sciubba DM, Burdette EC, Cheng JJ, Pennant WA, Noggle JC, Petteys RJ, et al. Percutaneous computed tomography fluoroscopy-guided conformal ultrasonic ablation of vertebral tumors in a rabbit tumor model: Laboratory investigation. Journal of Neurosurgery: Spine. 2010; 13(6):733–779.

23. Scott SJ, Prakash P, Salgaonkar V, Jones PD, Cam RN, Han M, et al. Approaches for modelling interstitial ultrasound ablation of tumours within or adjacent to bone: Theoretical and experimental evaluations. International Journal of Hyperthermia. 2013; 29(7):629–642. [PubMed: 24102393]

24. Scott SJ, Salgaonkar V, Prakash P, Burdette EC, Diederich CJ. Interstitial ultrasound ablation of vertebral and paraspinal tumours: Parametric and patient-specific simulations. International Journal of Hyperthermia. 2014; 30(4):228–244. [PubMed: 25017322]

25. Mast TD, Makin IRS, Faidi W, Runk MM, Barthe PG, Slayton MH. Bulk ablation of soft tissue with intense ultrasound: Modeling and experiments. The Journal of the Acoustical Society of America. 2005; 118(4):2715–2724. [PubMed: 16266191]

26. Prakash P, Salgaonkar VA, Burdette EC, Diederich CJ. Multiple applicator hepatic ablation with interstitial ultrasound devices: Theoretical and experimental investigation. Medical physics. 2012; 39(12):7338–7349. [PubMed: 23231283]

27. Deardorff DL, Diederich CJ. Angular directivity of thermal coagulation using air-cooled direct-coupled interstitial ultrasound applicators. Ultrasound in medicine & biology. 1999; 25(4):609–622. [PubMed: 10386737]

28. Deardorff DL, Diederich CJ. Axial control of thermal coagulation using a multi-element interstitial ultrasound applicator with internal cooling. Ultrasonics, Ferroelectrics and Frequency Control, IEEE Transactions on. 2000; 47(1):170–178.

29. Nau W, Diederich C, Stauffer P. Directional power deposition from direct-coupled and catheter-cooled interstitial ultrasound applicators. International journal of hyperthermia. 2000; 16(2):129–144. [PubMed: 10763742]

30. Delabrousse E, Mithieux F, Birer A, Chesnais S, Salomir R, Chapelon JY, et al. Percutaneous Sonographically Guided Interstitial US Ablation: Experimentation in an *In Vivo* Pig Liver Model. Journal of Vascular and Interventional Radiology. 2008; 19(12):1749–1756. [PubMed: 18952462]

31. Deardorff DL, Diederich CJ, Nau WH. Control of interstitial thermal coagulation: comparative evaluation of microwave and ultrasound applicators. Medical physics. 2001; 28(1):104–117. [PubMed: 11213915]

32. Prakash P, Diederich CJ. Considerations for theoretical modelling of thermal ablation with catheter-based ultrasonic sources: Implications for treatment planning, monitoring and control. International Journal of Hyperthermia. 2012; 28(1):69–86. [PubMed: 22235787]

33. Diederich C, Nau W, Burdette E, Bustany IK, Deardorff D, Stauffer P. Combination of transurethral and interstitial ultrasound applicators for high-temperature prostate thermal therapy. International journal of hyperthermia. 2000; 16(5):385–403. [PubMed: 11001573]

34. Nau W, Diederich C, Burdette E. Evaluation of multielement catheter-cooled interstitial ultrasound applicators for high-temperature thermal therapy. Medical physics. 2001; 28(7):1525–1534. [PubMed: 11488586]

35. Diederich CJ, Nau WH, Kinsey A, Ross T, Wootton J, Juang T, et al. Catheter-based ultrasound devices and MR thermal monitoring for conformal prostate thermal therapy. Engineering in

Medicine and Biology Society, 2008. :3664–3668. EMBS 2008. 30th Annual International Conference of the IEEE; 2008: IEEE; 2008.

36. Nau WH, Diederich CJ, Ross AB, Butts K, Rieke V, Bouley DM, et al. MRI-guided interstitial ultrasound thermal therapy of the prostate: a feasibility study in the canine model. Medical physics. 2005; 32(3):733–743. [PubMed: 15839345]

37. Stafford RJ, Price D, Roger E, Diederich CJ, Kangasniemi M, Olsson LE, et al. Interleaved echo-planar imaging for fast multiplanar magnetic resonance temperature imaging of ultrasound thermal ablation therapy. Journal of Magnetic Resonance Imaging. 2004; 20(4):706–714. [PubMed: 15390144]

38. Diederich, CJ.; Wootton, J.; Prakash, P.; Salgaonkar, V.; Juang, T.; Scott, S., et al. SPIE BiOS; 2011. International Society for Optics and Photonics; 2011. Catheter-based ultrasound hyperthermia with HDR brachytherapy for treatment of locally advanced cancer of the prostate and cervix; p. 79010O-79010O-8.

39. Wootton JH, Prakash P, Hsu ICJ, Diederich CJ. Implant strategies for endocervical and interstitial ultrasound hyperthermia adjunct to HDR brachytherapy for the treatment of cervical cancer. Physics in medicine and biology. 2011; 56(13):3967. [PubMed: 21666290]

40. Chen X, Diederich CJ, Wootton JH, Pouliot J, Hsu IC. Optimisation-based thermal treatment planning for catheter-based ultrasound hyperthermia. International Journal of Hyperthermia. 2010; 26(1):39–55. [PubMed: 20100052]

41. Salgaonkar VA, Prakash P, Diederich CJ. Temperature superposition for fast computation of 3D temperature distributions during optimization and planning of interstitial ultrasound hyperthermia treatments. International Journal of Hyperthermia. 2012; 28(3):235–249. [PubMed: 22515345]

42. Nau, WH., Jr; Diederich, CJ.; Simko, J.; Juang, T.; Jacoby, A.; Burdette, EC. Biomedical Optics (BiOS) 2007. 2007 International Society for Optics and Photonics; 2007. Ultrasound interstitial thermal therapy (USITT) for the treatment of uterine myomas; p. 64400F-64400F-8.

43. N'Djin W, Burtnyk M, Lipsman N, Bronskill M, Kucharczyk W, Schwartz M, et al. Active MR-temperature feedback control of dynamic interstitial ultrasound therapy in brain: In vivo experiments and modeling in native and coagulated tissues. Medical physics. 2014; 41(9):093301. [PubMed: 25186419]

44. Ross AB, Diederich CJ, Nau WH, Gill H, Bouley DM, Daniel B, et al. Highly directional transurethral ultrasound applicators with rotational control for MRI-guided prostatic thermal therapy. Physics in medicine and biology. 2004; 49(2):189. [PubMed: 15083666]

45. Pauly KB, Diederich CJ, Rieke V, Bouley D, Chen J, Nau WH, et al. Magnetic resonance-guided high-intensity ultrasound ablation of the prostate. Topics in Magnetic Resonance Imaging. 2006; 17(3):195–207. [PubMed: 17414077]

46. Hazle JD, Diederich CJ, Kangasniemi M, Price RE, Olsson LE, Stafford RJ. MRI-guided thermal therapy of transplanted tumors in the canine prostate using a directional transurethral ultrasound applicator. Journal of Magnetic Resonance Imaging. 2002; 15(4):409–417. [PubMed: 11948830]

47. Diederich C, Stafford R, Nau W, Burdette E, Price R, Hazle J. Transurethral ultrasound applicators with directional heating patterns for prostate thermal therapy: in vivo evaluation using magnetic resonance thermometry. Medical Physics. 2004; 31(2):405–413. [PubMed: 15000627]

48. Sommer G, Bouley D, Gill H, Daniel B, Pauly KB, Diederich C. Focal Ablation of Prostate Cancer: Four Roles for MRI Guidance. The Canadian journal of urology. 2013; 20(2):6672. [PubMed: 23587506]

49. Sommer G, Pauly KB, Holbrook A, Plata J, Daniel B, Bouley D, et al. Applicators for MR-Guided Ultrasonic Ablation of BPH. Investigative radiology. 2013; 48(6):387. [PubMed: 23462673]

50. Kinsey AM, Diederich CJ, Rieke V, Nau WH, Pauly KB, Bouley D, et al. Transurethral ultrasound applicators with dynamic multi-sector control for prostate thermal therapy: In vivo evaluation under MR guidance. Medical physics. 2008; 35(5):2081–2093. [PubMed: 18561684]

51. Wootton JH, Hsu ICJ, Diederich CJ. Endocervical ultrasound applicator for integrated hyperthermia and HDR brachytherapy in the treatment of locally advanced cervical carcinoma. Medical physics. 2011; 38(2):598–611. [PubMed: 21452697]

52. Ross AB, Diederich CJ, Nau WH, Rieke V, Butts RK, Sommer G, et al. Curvilinear transurethral ultrasound applicator for selective prostate thermal therapy. Medical physics. 2005; 32(6):1555–1565. [PubMed: 16013714]

53. Chopra R, Burtnyk M, Haider MA, Bronskill MJ. Method for MRI-guided conformal thermal therapy of prostate with planar transurethral ultrasound heating applicators. Physics in medicine and biology. 2005; 50(21):4957. [PubMed: 16237234]

54. Chopra R, Baker N, Choy V, Boyes A, Tang K, Bradwell D, et al. MRI-compatible transurethral ultrasound system for the treatment of localized prostate cancer using rotational control. Medical physics. 2008; 35(4):1346–1357. [PubMed: 18491529]

55. Chopra R, Colquhoun A, Burtnyk M, N'djin WA, Kobelevskiy I, Boyes A, et al. MR Imaging–controlled Transurethral Ultrasound Therapy for Conformal Treatment of Prostate Tissue: Initial Feasibility in Humans. Radiology. 2012; 265(1):303–313. [PubMed: 22929332]

56. Chopra R, Luginbuhl C, Foster FS, Bronskill MJ. Multifrequency ultrasound transducers for conformal interstitial thermal therapy. Ultrasonics, Ferroelectrics and Frequency Control, IEEE Transactions on. 2003; 50(7):881–889.

57. Lafon C, Koszek L, Chesnais S, Theillère Y, Cathignol D. Feasibility of a transurethral ultrasound applicator for coagulation in prostate. Ultrasound in medicine & biology. 2004; 30(1):113–122. [PubMed: 14962615]

58. Melodelima D, Salomir R, Chapelon JY, Theillère Y, Moonen C, Cathignol D. Intraluminal high intensity ultrasound treatment in the esophagus under fast MR temperature mapping: in vivo studies. Magnetic resonance in medicine. 2005; 54(4):975–982. [PubMed: 16155893]

59. Melodelima D, Prat F, Fritsch J, Theillere Y, Cathignol D. Treatment of esophageal tumors using high intensity intraluminal ultrasound: first clinical results. J Transl Med. 2008; 6:28. [PubMed: 18533990]

60. Rata M, Salomir R, Umathum R, Jenne J, Lafon C, Cotton F, et al. Endoluminal ultrasound applicator with an integrated RF coil for high-resolution magnetic resonance imaging-guided high-intensity contact ultrasound thermotherapy. Physics in medicine and biology. 2008; 53(22):6549. [PubMed: 19205075]

61. Rata M, Birlea V, Murillo A, Paquet C, Cotton F, Salomir R. Endoluminal MR-guided ultrasonic applicator embedding cylindrical phased-array transducers and opposed-solenoid detection coil. Magnetic Resonance in Medicine. 2014

62. Pioche M, Lafon C, Constanciel E, Vignot A, Birer A, Gincul R, et al. High-intensity focused ultrasound liver destruction through the gastric wall under endoscopic ultrasound control: first experience in living pigs. Endoscopy. 2012; 44(S 02):E376–E377. [PubMed: 23012031]

63. Constanciel E, N'djin W, Bessiere F, Chavrier F, Grinberg D, Vignot A, et al. Design and evaluation of a transesophageal HIFU probe for ultrasound-guided cardiac ablation: simulation of a HIFU mini-maze procedure and preliminary ex vivo trials. IEEE transactions on ultrasonics, ferroelectrics, and frequency control. 2013; 60(9):1868–1883.

64. Couppis A, Damianou C, Kyriacou P, Lafon C, Chavrier F, Chapelon JY, et al. Heart ablation using a planar rectangular high intensity ultrasound transducer and MRI guidance. Ultrasonics. 2012; 52(7):821–829. [PubMed: 22525419]

65. Diederich C, Salgaonkar V, Prakash P, Adams M, Scott S, Jones P, et al. Catheter-based and endoluminal ultrasound applicators for magnetic resonance image-guided thermal therapy of pancreatic cancer: Preliminary investigations. The Journal of the Acoustical Society of America. 2013; 134(5):4089–4089.

66. Prakash, P.; Salgaonkar, VA.; Scott, SJ.; Jones, P.; Hensley, D.; Holbrook, A., et al. SPIE BiOS. 2013: International Society for Optics and Photonics; 2013. MR guided thermal therapy of pancreatic tumors with endoluminal, intraluminal and interstitial catheter-based ultrasound devices: preliminary theoretical and experimental investigations; p. 85840V-85840V-10.

67. Melodelima D, Salomir R, Mougenot C, Moonen C, Cathignol D. 64-element intraluminal ultrasound cylindrical phased array for transesophageal thermal ablation under fast MR temperature mapping: an ex vivo study. Medical physics. 2006; 33(8):2926–2934. [PubMed: 16964871]

68. Yin X, Epstein LM, Hynynen K. Noninvasive transesophageal cardiac thermal ablation using a 2-D focused, ultrasound phased array: a simulation study. Ultrasonics, Ferroelectrics and Frequency Control, IEEE Transactions on. 2006; 53(6):1138–1149.

69. Pichardo S, Hynynen K. Circumferential lesion formation around the pulmonary veins in the left atrium with focused ultrasound using a 2D-array endoesophageal device: a numerical study. Physics in medicine and biology. 2007; 52(16):4923. [PubMed: 17671344]

70. Pichardo S, Hynynen K. New design for an endoesophageal sector-based array for the treatment of atrial fibrillation: a parametric simulation study. Ultrasonics, Ferroelectrics and Frequency Control, IEEE Transactions on. 2009; 56(3):600–612.

71. Lee H, Francischelli D, Smith NB. Design of Focused Ultrasound Array for Non-Invasive Transesophageal Cardiac Ablation. Open Medical Devices Journal. 2010; 2:51–60.

72. Werner J, Park EJ, Lee H, Francischelli D, Smith NB. Feasibility of *in vivo* Transesophageal Cardiac Ablation Using a Phased Ultrasound Array. Ultrasound in medicine & biology. 2010; 36(5):752–760. [PubMed: 20347517]

73. Wootton JH, Ross AB, Diederich CJ. Prostate thermal therapy with high intensity transurethral ultrasound: The impact of pelvic bone heating on treatment delivery. International Journal of Hyperthermia. 2007; 23(8):609–622. [PubMed: 18097849]

74. Burtnyk M, Chopra R, Bronskill MJ. Quantitative analysis of 3-D conformal MRI-guided transurethral ultrasound therapy of the prostate: Theoretical simulations. International Journal of Hyperthermia. 2009; 25(2):116–131. [PubMed: 19337912]

75. Goharrizi AY, N'djin WA, Kwong R, Chopra R. Development of a new control strategy for 3D MRI-controlled interstitial ultrasound cancer therapy. Medical physics. 2013; 40(3):033301. [PubMed: 23464342]

76. Schmitt A, Mougenot C, Chopra R. Spatiotemporal filtering of MR-temperature artifacts arising from bowel motion during transurethral MR-HIFU. Medical physics. 2014; 41(11):113302. [PubMed: 25370670]

77. Yazdanpanah Goharrizi A, Kwong R, Chopra R. Development of robust/predictive control strategies for image-guided ablative treatments using a minimally invasive ultrasound applicator. International Journal of Hyperthermia. 2014; (0):1–9. [PubMed: 24350642]

78. Yazdanpanah A, Kwong R, Chopra RA. A Self-Tuning Adaptive Controller for 3D Image-Guided Ultrasound Cancer Therapy. 2014

79. N'djin WA, Burtnyk M, Bronskill M, Chopra R. Investigation of power and frequency for 3D conformal MRI-controlled transurethral ultrasound therapy with a dual frequency multi-element transducer. International Journal of Hyperthermia. 2012; 28(1):87–104. [PubMed: 22235788]

80. Chen J, Daniel BL, Diederich CJ, Bouley DM, van den Bosch MA, Kinsey AM, et al. Monitoring prostate thermal therapy with diffusion-weighted MRI. Magnetic Resonance in Medicine. 2008; 59(6):1365–1372. [PubMed: 18506801]

81. Kinsey AM, Diederich CJ, Tyreus PD, Nau WH, Rieke V, Pauly KB. Multisectored interstitial ultrasound applicators for dynamic angular control of thermal therapy. Medical physics. 2006; 33(5):1352–1363. [PubMed: 16752571]

82. Partanen A, Yerram NK, Trivedi H, Dreher MR, Oila J, Hoang AN, et al. Magnetic resonance imaging (MRI)-guided transurethral ultrasound therapy of the prostate: a preclinical study with radiological and pathological correlation using customised MRI-based moulds. BJU international. 2013; 112(4):508–516. [PubMed: 23746198]

83. Melodelima D, Lafon C, Prat F, Theillère Y, Arefiev A, Cathignol D. Transoesophageal ultrasound applicator for sector-based thermal ablation: first *in vivo* experiments. Ultrasound in medicine & biology. 2003; 29(2):285–291. [PubMed: 12659916]

84. Prat F, Lafon C, Margonari J, Gorry F, Theillère Y, Chapelon JY, et al. A high-intensity US probe designed for intraductal tumor destruction: experimental results. Gastrointestinal endoscopy. 1999; 50(3):388–392. [PubMed: 10462662]

85. Lafon C, Theillere Y, Prat F, Arefiev A, Chapelon J, Cathignol D. Development of an interstitial ultrasound applicator for endoscopic procedures: animal experimentation. Ultrasound in medicine & biology. 2000; 26(4):669–675. [PubMed: 10856631]

86. Constanciel E, N'Djin W, Bessière F, Pioche M, Chevalier P, Chapelon JY, et al. Ultrasound-guided transesophageal HIFU exposures for atrial fibrillation treatment: First animal experiment. IRBM. 2013; 34(4):315–318.

87. He D, Zimmer J, Hynynen K, CARCUS F, Caruso A, Lampe L, et al. Application of ultrasound energy for intracardiac ablation of arrhythmias. European heart journal. 1995; 16(7):961–966. [PubMed: 7498212]

88. Hynynen K, Dennie J, Zimmer JE, Simmons WN, He DS, Marcus FI, et al. Cylindrical ultrasonic transducers for cardiac catheter ablation. Biomedical Engineering, IEEE Transactions on. 1997; 44(2):144–151.

89. Lesh M, Diederich C, Guerra P, Goseki Y, Sparks P. An anatomic approach to prevention of atrial fibrillation: pulmonary vein isolation with through-the-balloon ultrasound ablation (TTB-USA). The Thoracic and cardiovascular surgeon. 1999; 47(S 3):347–351. [PubMed: 10520766]

90. Meininger GR, Calkins H, Lickfett L, Lopath P, Fjield T, Pacheco R, et al. Initial experience with a novel focused ultrasound ablation system for ring ablation outside the pulmonary vein. Journal of interventional cardiac electrophysiology. 2003; 8(2):141–148. [PubMed: 12766506]

91. Natale A, Pisano E, Shewchik J, Bash D, Fanelli R, Potenza D, et al. First human experience with pulmonary vein isolation using a through-the-balloon circumferential ultrasound ablation system for recurrent atrial fibrillation. Circulation. 2000; 102(16):1879–1882. [PubMed: 11034932]

92. Saliba W, Wilber D, Packer D, Marrouche N, Schweikert R, Pisano E, et al. Circumferential ultrasound ablation for pulmonary vein isolation: analysis of acute and chronic failures. Journal of cardiovascular electrophysiology. 2002; 13(10):957–961. [PubMed: 12435178]

93. Sinelnikov Y, Fjield T, Sapozhnikov O. The mechanism of lesion formation by focused ultrasound ablation catheter for treatment of atrial fibrillation. Acoustical physics. 2009; 55(4-5):647–656. [PubMed: 20161431]

94. Schmidt B, Chun KJ, Kuck KH, Antz M. Pulmonary vein isolation by high intensity focused ultrasound. Indian pacing and electrophysiology journal. 2007; 7(2):126. [PubMed: 17538703]

95. Schmidt B, Antz M, Ernst S, Ouyang F, Falk P, Chun JK, et al. Pulmonary vein isolation by high-intensity focused ultrasound: first-in-man study with a steerable balloon catheter. Heart Rhythm. 2007; 4(5):575–584. [PubMed: 17467623]

96. Nakagawa H, Antz M, Wong T, Schmidt B, Ernst S, Ouyang F, et al. Initial Experience Using a Forward Directed, High-Intensity Focused Ultrasound Balloon Catheter for Pulmonary Vein Antrum Isolation in Patients with Atrial Fibrillation. Journal of cardiovascular electrophysiology. 2007; 18(2):136–144. [PubMed: 17239138]

97. Gentry KL, Palmeri ML, Sachedina N, Smith SW. Finite-element analysis of temperature rise and lesion formation from catheter ultrasound ablation transducers. Ultrasonics, Ferroelectrics and Frequency Control, IEEE Transactions on. 2005; 52(10):1713–1721.

98. Mabin T, Sapoval M, Cabane V, Stemmett J, Iyer M. First experience with endovascular ultrasound renal denervation for the treatment of resistant hypertension. EuroIntervention. 2012; 8(1):57–61. [PubMed: 22580249]

99. Sakakura K, Roth A, Ladich E, Shen K, Coleman L, Joner M, et al. Controlled circumferential renal sympathetic denervation with preservation of the renal arterial wall using intraluminal ultrasound: a next-generation approach for treating sympathetic overactivity. EuroIntervention: journal of EuroPCR in collaboration with the Working Group on Interventional Cardiology of the European Society of Cardiology. 2014

100. Neven K, Metzner A, Schmidt B, Ouyang F, Kuck KH. Two-year clinical follow-up after pulmonary vein isolation using high-intensity focused ultrasound (HIFU) and an esophageal temperature-guided safety algorithm. Heart Rhythm. 2012; 9(3):407–413. [PubMed: 21978960]

101. Garcia R, Sacher F, Oses P, Derval N, Barandon L, Denis A, et al. Electrophysiological study 6 months after Epicor™ high-intensity focused ultrasound atrial fibrillation ablation. Journal of Interventional Cardiac Electrophysiology. 2014:1–7.

102. Davies EJ, Bazerbashi S, Asopa S, Haywood G, Dalrymple-Hay M. Long-Term Outcomes Following High Intensity Focused Ultrasound Ablation for Atrial Fibrillation. Journal of cardiac surgery. 2014; 29(1):101–107. [PubMed: 24387128]

103. Koruth JS, Dukkipati S, Carrillo RG, Coffey J, Teng J, Eby TB, et al. Safety and Efficacy of High-Intensity Focused Ultrasound Atop Coronary Arteries During Epicardial Catheter Ablation. Journal of cardiovascular electrophysiology. 2011; 22(11):1274–1280. [PubMed: 21676047]

104. Bhatt DL, Kandzari DE, O'Neill WW, D'Agostino R, Flack JM, Katzen BT, et al. A controlled trial of renal denervation for resistant hypertension. New England Journal of Medicine. 2014; 370(15):1393–1401. [PubMed: 24678939]

105. Burdette, EC.; Banovac, F.; Diederich, CJ.; Cheng, P.; Wilson, E.; Cleary, KR. SPIE BiOS 2011. International Society for Optics and Photonics; 2011. Conformal needle-based ultrasound ablation using EM-tracked conebeam CT image guidance; p. 790107-790107-9.

106. Boctor, EM.; Stolka, P.; Kang, HJ.; Clarke, C.; Rucker, C.; Croom, J., et al. SPIE Medical Imaging; 2010. International Society for Optics and Photonics; 2010. Precisely shaped acoustic ablation of tumors utilizing steerable needle and 3D ultrasound image guidance; p. 76252N-76252N-10.

107. Imani F, Abolmaesumi P, Wu MZ, Lasso A, Burdette EC, Ghoshal G, et al. Ultrasound-guided characterization of interstitial ablated tissue using RF time series: feasibility study. IEEE Trans Biomed Engineering. 2013; 60(6):1608–1618.

108. Burdette, EC.; Rucker, DC.; Prakash, P.; Diederich, CJ.; Croom, JM.; Clarke, C., et al. SPIE Medical Imaging; 2010. International Society for Optics and Photonics; 2010. The ACUSITT ultrasonic ablator: the first steerable needle with an integrated interventional tool; p. 76290V-76290V-10.

109. Boctor EM, Choti MA, Burdette EC, Webster Iii RJ. Three-dimensional ultrasound-guided robotic needle placement: an experimental evaluation. The International Journal of Medical Robotics and Computer Assisted Surgery. 2008; 4(2):180–191. [PubMed: 18433079]

110. Mangrum JM, Mounsey JP, Kok LC, DiMarco JP, Haines DE. Intracardiac echocardiography-guided, anatomically based radiofrequency ablation of focal atrial fibrillation originating from pulmonary veins. Journal of the American College of Cardiology. 2002; 39(12):1964–1972. [PubMed: 12084595]

111. Delabrousse E, Salomir R, Birer A, Paquet C, Mithieux F, Chapelon JY, et al. Automatic temperature control for MR-guided interstitial ultrasound ablation in liver using a percutaneous applicator: Ex vivo and in vivo initial studies. Magnetic Resonance in Medicine. 2010; 63(3):667–679. [PubMed: 20187177]

112. Hynynen K. MRIgHIFU: A tool for image-guided therapeutics. Journal of Magnetic Resonance Imaging. 2011; 34(3):482–493. [PubMed: 22896850]

113. Pisani LJ, Ross AB, Diederich CJ, Nau WH, Sommer FG, Glover GH, et al. Effects of spatial and temporal resolution for MR image-guided thermal ablation of prostate with transurethral ultrasound. Journal of Magnetic Resonance Imaging. 2005; 22(1):109–118. [PubMed: 15971190]

114. Ramsay E, Mougenot C, Köhler M, Bronskill M, Klotz L, Haider MA, et al. MR thermometry in the human prostate gland at 3.0 T for transurethral ultrasound therapy. Journal of Magnetic Resonance Imaging. 2013; 38(6):1564–1571. [PubMed: 23440850]

115. Rieke V, Butts Pauly K. MR thermometry. Journal of Magnetic Resonance Imaging. 2008; 27(2):376–390. [PubMed: 18219673]

116. Grissom WA, Rieke V, Holbrook AB, Medan Y, Lustig M, Santos J, et al. Hybrid referenceless and multibaseline subtraction MR thermometry for monitoring thermal therapies in moving organs. Medical physics. 2010; 37(9):5014–5026. [PubMed: 20964221]

117. Roujol S, Ries M, Quesson B, Moonen C, Denis de Senneville B. Real-time MR-thermometry and dosimetry for interventional guidance on abdominal organs. Magnetic Resonance in Medicine. 2010; 63(4):1080–1087. [PubMed: 20373409]

118. Gellermann J, Wlodarczyk W, Feussner A, Fähling H, Nadobny J, Hildebrandt B, et al. Methods and potentials of magnetic resonance imaging for monitoring radiofrequency hyperthermia in a hybrid system. International journal of hyperthermia. 2005; 21(6):497–513. [PubMed: 16147436]

119. Gellermann J, Wlodarczyk W, Ganter H, Nadobny J, Fähling H, Seebass M, et al. A practical approach to thermography in a hyperthermia/magnetic resonance hybrid system: Validation in a heterogeneous phantom. International Journal of Radiation Oncology* Biology* Physics. 2005; 61(1):267–277.

120. Weihrauch M, Wust P, Weiser M, Nadobny J, Eisenhardt S, Budach V, et al. Adaptation of antenna profiles for control of MR guided hyperthermia (HT) in a hybrid MR-HT system. Medical physics. 2007; 34:4717. [PubMed: 18196799]

121. Stauffer, P.; Craciunescu, OI.; Maccarini, P.; Wyatt, C.; Arunachalam, K.; Arabe, O., et al. SPIE BiOS: Biomedical Optics; 2009. International Society for Optics and Photonics; 2009. Clinical utility of magnetic resonance thermal imaging (MRTI) for realtime guidance of deep hyperthermia; p. 71810I-71810I-12.

122. Craciunescu OI, Stauffer PR, Soher BJ, Wyatt CR, Arabe O, Maccarini P, et al. Accuracy of real time noninvasive temperature measurements using magnetic resonance thermal imaging in patients treated for high grade extremity soft tissue sarcomas. Medical physics. 2009; 36:4848. [PubMed: 19994492]

123. Lepetit-Coiffé M, Laumonier H, Seror O, Quesson B, Sesay MB, Moonen CT, et al. Real-time monitoring of radiofrequency ablation of liver tumors using thermal-dose calculation by MR temperature imaging: initial results in nine patients, including follow-up. European radiology. 2010; 20(1):193–201. [PubMed: 19657650]

124. Sanghvi NT, Morris A. Laparoscopic high intensity focused ultrasound for the treatment of soft tissue. The Journal of the Acoustical Society of America. 2013; 134(5):4180–4180.

125. Prat F, Lafon C, de Lima DM, Theilliere Y, Fritsch J, Pelletier G, et al. Endoscopic treatment of cholangiocarcinoma and carcinoma of the duodenal papilla by intraductal high-intensity US: Results of a pilot study. Gastrointestinal endoscopy. 2002; 56(6):909–915. [PubMed: 12447312]
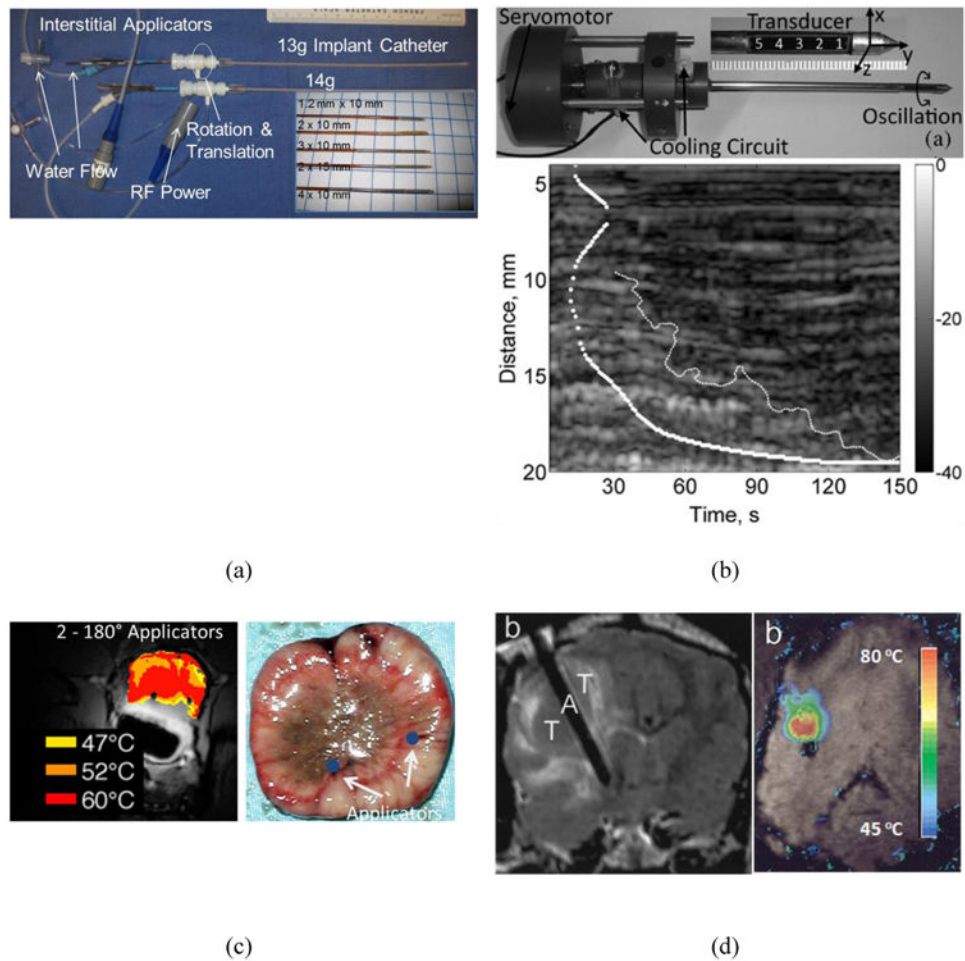
(a)

(b)

(c)

(d)

Figure 1.

Sub-figure panels include examples showing selected applications of interstitial CBUS from multiple studies. (a) Prototypes of interstitial devices with sectored tubular transducers with 13-g, 14-g delivery catheters; these catheters are also used in HDR brachytherapy [38]. (b) Photograph of single-element dual-mode ultrasound applicator prototype, and an M-mode image created by the same applicator showing hypoechoic region corresponding to ablation [17, 18]. (c) Example of MR thermometry during interstitial ablation of prostate (*in vivo* canine) with multiple devices, and post-procedure histology showing good correlation between localized tissue damage and temperature maps. [36]. (d) Example of brain tumor ablation and MRTI with an interstitial applicator in a canine subject *in vivo* to illustrate image-guided device placement and real-time thermometry[10].
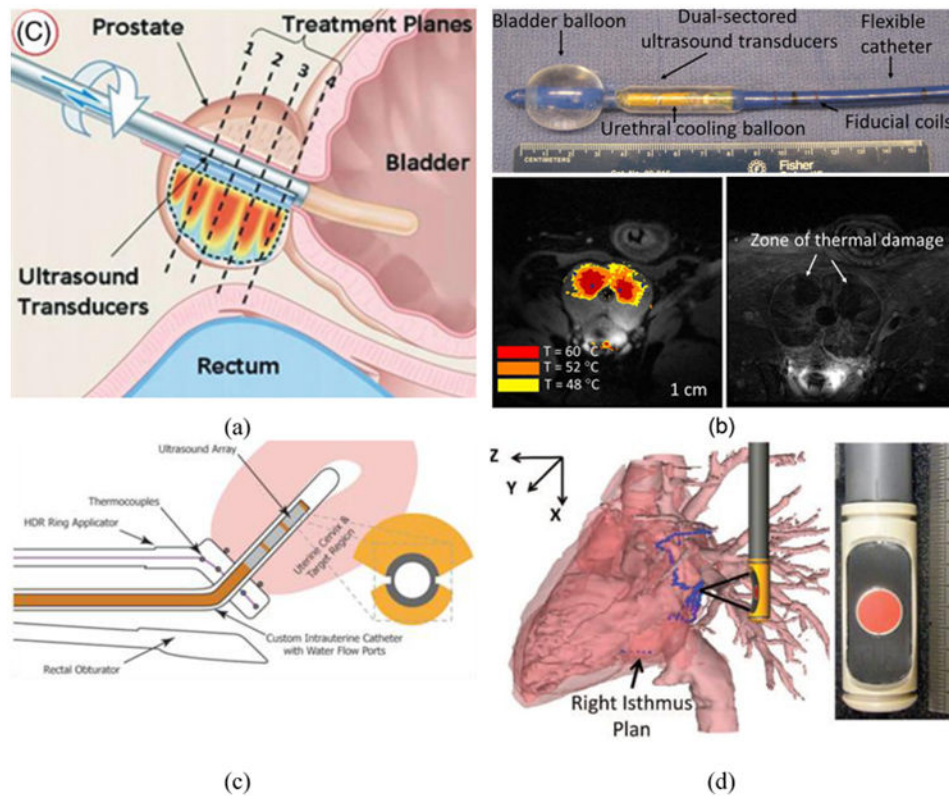
Figure 2.
This figure shows four examples of endoluminal applicators. (a) Schematic showing a transurethral applicator with multiple planar elements for prostate cancer ablation under MRTI [55]. (b) Example of transurethral prostate ablation for BPH treatment with a multi-sectored tubular transurethral device under MRTI and post ablation CE-MRI in a canine subject *in vivo* demonstrating selective targeting of transition zone in the prostate[49]. (c) Schematic of a bi-directional endocervical applicator with sectored tubular transducers integrated within a tandem holder used in clinical HDR brachytherapy [51]. (d) Prototype for a transesophageal cardiac ablation applicator with a large HIFU treatment array and central imaging transducer.
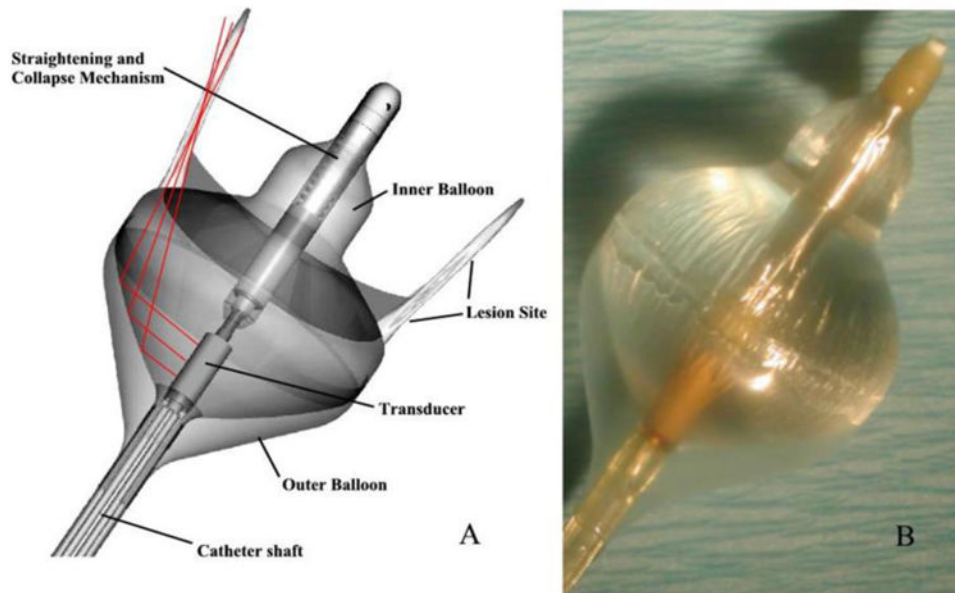
Figure 3.
Schematic (left panel) and prototype (right panel) of a tip-firing cardiac ablation catheter
designed for treating atrial fibrillation by ablating tissue around the pulmonary vein
circumference. Here, acoustic energy generated by the cylindrical transducer element is
reflected by the air-water interface created by the outer air-filled balloon and the inner
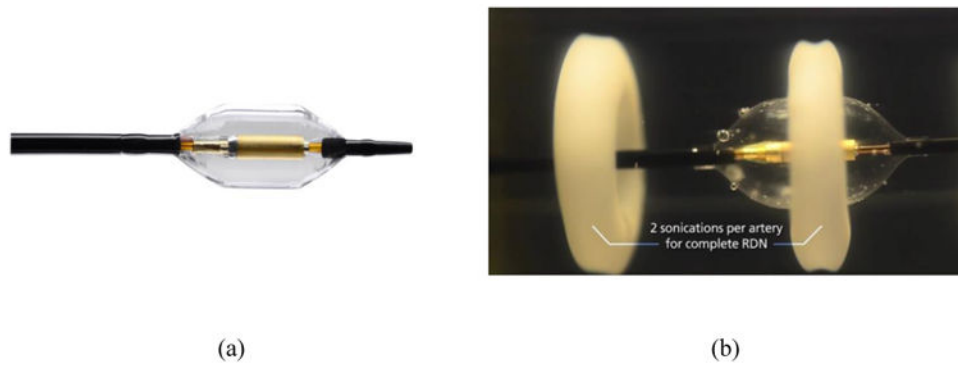water-filled coupling balloon.

(a)

(b)

Figure 4.
(a) Prototype of a renal denervation device designed for circumferential ablation of nerves surrounding the renal artery [Image courtesy Recor Medical, Palo Alto, CA]. (b) Circumferential ablation demonstrated in a gel phantom by the same device [Image courtesy Recor Medical, Palo Alto, CA].

Table 1

Summary of selected interstitial CBUS devices, their design features, performance evaluations and clinical utilizations.

CBUS Device	General Design Features	Performance	Site-Specific Evaluations	Clinical Utilization
Interstitial: sectored tubular arrays	Multiple sectored tubular transducer array; 6 -8 MHz; 10 – 15 mm segments; 1.5 – 2.4 mm OD; Sector-based angular control; integratedcatheter or internal cooling	Lesion dimensions 15-20 mm radial, 10 – 40 mm length; Ablation and HT; MRTI, CT, US, Fluoroscopy guidance	*in vivo* canine brain [10, 37] and prostate [36], porcine liver [31] ovine [21] and rabbit spine [22]	Prostate and cervix hyperthermia with HDR brachytherapy [38]
Interstitial: multi-faced	7-sided catheter assembly w/ array of 1 mm × 1mm transducers; 6 MHz; 8 mm active length; OD = 3.2 mm; angular control through power activation on each face; external cooling sheath	Radial treatment depth > 15 mm; MR-compatible with MRTI in 1.5 T	Brain [11]	
Interstitial & Intraductal rotating planar	3.8-4 mm OD catheter, 8-10 mm length × 2.8-3.0 mm planar transducer segment, ~5 or 10 MHz, motorized rotation; integrated cooling sheath	~20 mm radial × 8 mm length penetration, rotation for angular control; endoscopic intraluminal or interstitial; fluoroscopy or US guidance.	Porcine biliary tract [84, 85] and liver [30, 84]	Bile duct carcinoma [125]
Interstitial: dual-mode	Dual-mode linear array, 32 rect. Elements, 2.3 × 49 mm²; 3.1 or 4.8 MHz; motorized rotational control; balloon cooling	Lesion dimensions ~ 18 mm radial,~ 5 mm wide, and ~ 15 mm length; Dual-mode with US B-mode imaging	in vivo rabbit liver [14, 15]	
Interstitial: dual-mode w/ mechanical rotation	Dual-mode linear array; 5 rect. elements, 3 × 20 mm², 5 - 6 MHz, cylindrical focus ~ 14 mm; motorized rotational control; balloon cooling	Lesion dimensions 19 mm depth, ~9 mm wide; dual-mode with US therapy with all 5 elements, B-mode imaging with central transducer	Porcine liver in vivo [18]	

Table 2

Summary of selected endoluminal CBUS devices, their design features, performance evaluations and clinical utilizations.

CBUS Device	General Design Features	Performance	Site-Specific Evaluations	Clinical Utilization
Endoluminal: sectored tubular arrays	Transurethral or endocervical configurations; Multi-sectored tubular transducers, 6 -8 MHz, 6-10 mm length segments, 2.5-3.5 mm OD transducers; sector-based angular control; cooling balloon or sheath	Transurethral prostate lesion dimensions 15-20 mm radial, 90-120 deg. sectors, × 6-30 mm length; endocervical hyperthermia ~ 20 mm radial, 180 or 120 deg sectors, × 20-30 mm length	Prostate: Canine in vivo for treating BPH or focal cancer [50]	Cervix Hyperthermia w/HDR brachytherapy [38, 51]
Endoluminal: planar, rotating	Transurethral configuration w/ linear array, 1-8 rect., 4.7 and/or 9.7 MHz [dual frequency]; 20 – 40 mm length × 4 mm wide, 6 mm OD; Motorized rotational control; integrated cooling sheath and membrane	Penetration depth ~ 20 mm; Integrated with MRTI-based feedback control; lesion depth control over rotation; +/- 1 mm conformal target boundary	Prostate: canine in vivo [82]	Prostate cancer ablation [55]
Endoluminal: planar with integrated US imaging	Single rect. therapy transducer, 10 MHz; single rect. imaging element, 12 MHz; 10 mm OD for esophageal placement; Imaging probe can be deployed and retracted through a channel within the device; Motorized rotational control	Penetration depth ~ 10 mm; integrated US imaging for guidance	Esophagus: swine in vivo [83]	Esophageal tumors[59]

Table 3

Summary of selected endovascular CBUS devices, their design features, performance evaluations and clinical utilizations.

CBUS Device	General Design Features	Performance	Site-Specific Evaluations	Clinical Utilization
Endovascular: pulmonary vein isolation	Endocardial access for placement within pulmonary vein; single tubular transducer, 6 - 8 MHz; Delivery catheter: 2.7-4.7 mm OD; Cooling balloon; multi-chamber balloon w/parabolic reflector.	Penetration depth ∼ 6 mmCT/ Fluoroscopic guidance during endocardial access.	Ablation of tissue around pulmonary vein ostium: *in vivo* canine [90]	Treatment of atrial fibrillation [91, 95, 96]
Endovascular: renal denervation	Configured for vascular placement within renal artery; 360 deg tubular transducer, 1mm OD × 6 mm long transducer, 8-9 MHz; 2 mm OD catheter w/6 mm expandable cooling balloon	Penetration depth ∼ 7 - 10 mm × 360 deg., with sparing of renal artery; fluoroscopic guidance;	Ablation of sympathetic nerves surrounding renal artery, decrease in blood pressure; In vivo porcine [99]	Treatment of resistant hypertension [98]